

# A Proposal for Bad-Cavity Optomechanical Ground-State Cooling Via Coupling to a Parity-Time Symmetric Cavity

Zohre Mahmoudi Meimand<sup>a,\*</sup>, Omid Hamidi<sup>a</sup>, and Ali Reza Bahrampour<sup>b</sup>

<sup>a</sup>Department of Physics, University of Shahid Bahonar of Kerman, Kerman, Iran

<sup>b</sup>Department of Physics, Sharif University, Tehran, Iran

\*Corresponding author email: [zohre.mm@gmail.com](mailto:zohre.mm@gmail.com)

Regular paper: Received: Feb. 05, 2023, Revised: Apr. 01, 2023, Accepted: Apr. 04, 2023,  
Available Online: Apr. 06, 2023, DOI: 10.52547/ijop.16.2.161

**Abstract—** In This paper a ground-state cooling method for bad optomechanical systems is proposed. Previous authors show that an optical cavity with equal loss and gain has a parity-time reversal (PT) symmetry. We introduced an optomechanical cavity coupled to the two modes of a PT symmetry and a passive optical cavity. A quarter-wave plate provides linear mixing interaction between the PT symmetry and passive cavities. In this study, our proposed system improved the cooling rate by utilizing two effects: energy localization and quantum interference. These two impacts increase the cooling rate while the system is red or blue-detuned. It is demonstrated that optomechanical cooling occurs in both the bad-cavity limit and the weak optomechanical coupling regime. These innovations can be attained by parameter management of the system.

**KEYWORDS:** Ground State Cooling, Optomechanical System, Parity-Time Symmetric, Quantum Interference.

## I. INTRODUCTION

Ground-state cooling optomechanical systems are excellent tools for fundamental quantum experiments and quantum technologies [1-5]. In optomechanical systems, the radiation pressure causes the photon-phonon interaction. The photon-phonon interaction provides stokes and anti-stokes scattering. The generation of stokes and anti-stokes frequencies is due to the creation and annihilation of mirror phonons, respectively. The rate of the phonon annihilation is computed by the differences

between the stokes and anti-stokes amplitude. This can be engineered using the optomechanical cavity spectrum. There are general dissipative and dispersive methods for mechanical mode cooling [6]-[8]. In dispersive cooling methods, the amplitude of the normalized spectrum at the anti-stokes frequency is much greater than stokes [9]. However, in the dissipative method, the absorption is frequency-dependent, and the stokes frequency is much larger than the anti-stokes frequency. In addition to dispersive and dissipative cooling methods, the sympathetic cooling method can be employed. Light can be used to mediate heat transfer from a hot mirror or nano-particle to the ultra-cold atoms [10]. The most famous dispersive method is the resolved sideband cooling [11-12]. The resolved sideband method can be employed in a good cavity optomechanical system, where the mechanical frequency is much greater than the cavity decay rate  $k \ll \omega_m$ . Theoretically, it is predicted that the average phonon number of the cooled mirror is proportional to the square of  $\omega_m$  and the cooling rate is proportional to cavity decay rate [6].

For a small mechanical frequency, the cooling is inefficient and the cooling rate is minimal. Outside the resolved-sideband regime, approaches to the ground state cooling have been proposed, e.g., the dissipative coupling mechanism [13], hybrid systems [14], and electromagnetically induced transparency

(EIT) cooling [15]. The interference effects in systems, including the optomechanical cavity and one or more auxiliary cavities, could improve the cooling efficiency.

In [16], the authors have considered an optomechanical cooling system consisting of a two-mode optical cavity. Two cavity modes are orthogonally polarized, and a quarter-wave plate inside the cavity provides the linear mixing interaction between these two modes. In this paper, a fast ground state optomechanical cooling is proposed. Therefore, the destructive quantum interference between the two-cavity modes, using the quarter-wave plate, helps to suppress the heating process. Another method for cooling is applying. Exceptional points in parity time reversal (PT)-symmetry [17] and in the optomechanical cavity has been discussed in many papers, e.g., non-reciprocal energy or state transfer [18] phonon laser [19] and chaos [20]. Also, the PT-symmetric gain-loss cavities coupled to an optomechanical system have a long range of the applications [21]. In some recent works, the mechanical cooling using PT symmetry has been studied [22]. In this paper, the proposed system consists of the gain cavity, which is coupled to the optomechanical cavity and also, there exists the quarter-wave plate that provides the linear mixing between the optomechanical and the PT symmetric optical cavity. The results demonstrate that the cooling rate is increased by two main reasons. Energy localization in gain cavity near the exceptional point and the interference affects which both of them eliminate the heat process. In the proposed method, the cooling rate increase even in the bad cavity system.

The remaining part of the paper is organized as follow. The theoretical method is presented in section A. The linearized equations are given in section B. In section D, numerical calculation and the results can be seen. The paper is then finished with some calculations.

## II. THEORETICAL MODEL

As shown in Fig. 1, we consider an optomechanical system consisting of a two-mode optical cavity. The two-mode optical cavity constructed from three fixed mirrors M2,

M3 and M4 and one moving mirror M1 which is allowed to oscillate under the radiation pressure of inter cavity light pressure. An active-passive cavity is the (M1-M3) cavity The active medium is located between the M2 and M3 mirrors while (M1-M2) is a passive cavity. It is shown that in an optical cavity with equal gain and loss, the system has PT symmetry, which have interesting property. For example, in a system of active and passive medium the energy flows from the active to the passive one, where in PT-symmetry optomechanical system the phonon energy of mechanical resonator through the passive part transfer to the active medium and localized in the active medium [22]-[27]. This effect causes to enhance the heat transfer and spring effect i.e., a shift in mechanical resonator frequency and an increase in the damping rate occurs. Furthermore, the quarter wave plate QWP placed inside the cavity, causes linear mixing interaction between the (M1-M3) and (M1-M4) cavity modes. (M1-M4) and (M1-M3) cavities are excited by two lasers with the same frequencies and orthogonal polarization. Suppose the cavity bandwidth of (M1-M3) is much greater than that of (M1-M4) cavity. The (M1-M4) is designed for resolved sideband cooling and (M1-M3) is suitable for high-rate heat transfer. The collaboration of field localization and band width enhancement causes the enhancement of cooling rate; relative to the previous works. In previous publications [16] on the basis of good cavity assumptions ( $k_1 \gg k_2$ ) it is shown that cooling rate, two order of magnitude is greater than the conventional resolved sideband cooling. In this paper we show that in the presence of PT symmetry even in a bad cavity system enhanced cooling rate relative to the good cavity system is obtained.

The effective Hamiltonian of the full system becomes  $H = H_0 + H_I$  which  $H_0$  is free part, and  $H_I$  is the interaction part of the effective Hamiltonian. In a system of units where  $\hbar = 1$ , the Hamiltonian  $H_0$  is

$$H_0 = \sum_{j=1}^3 (\omega_j a_j^\dagger a_j) + \omega_m b^\dagger b, \quad (1)$$

where  $\omega_j$  and  $a_j$ ,  $j=1,2,3$  are frequencies and annihilation bosonic operators of the  $j$ th cavity, respectively. The mechanical resonator is depicted by bosonic annihilation and creation operators  $b$  and  $b^\dagger$  with the frequency  $\omega_m$ . The first three terms on the right-hand side of Eq. 1 are the energy of the cavities in optical mode, and the last term is due to the energy of a mechanical oscillator. The last term of the effective Hamiltonian is the interaction term

$$H_1 = \sum_{j=1}^2 G_j a_j^\dagger a_j (b + b^\dagger) + i \frac{g}{2} (a_2 a_1^\dagger - a_1 a_2^\dagger) + J (a_1^\dagger a_3 + a_1 a_3^\dagger) + \sum_{j=2}^3 \Omega_j (a_j + a_j^\dagger). \quad (2)$$

The first term on the right-hand side of Eq. 2 is the radiation pressure, interaction with moving mirror. Here,  $G_j = G_0 \alpha_j$ ,  $j=1,2$  is the coherent driving enhanced optomechanical coupling strength and  $G_0$  is single-photon mirror optomechanical coupling coefficient.

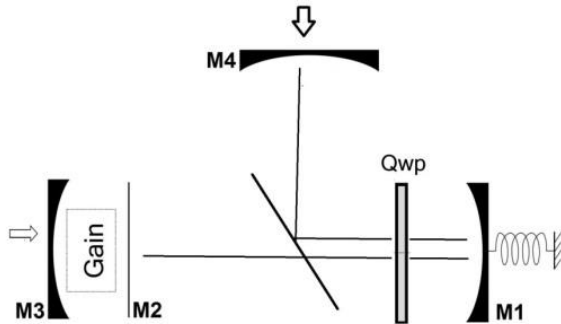


Fig. 1. Schematic diagram of an optomechanical system comprising of the gain-loss system (M1-M3) coupled to the cavity (M1-M4). An active optical mode  $a_3$  with gain  $k_3$  in a gain cavity (M2-M3) is coupled to a passive optical mode  $a_1$  with decay rate  $k_1$  in the optomechanical cavity (M1-M2) and form the PT-symmetric system (M1-M3). A passive optical mode  $a_2$  in a loss cavity (M1-M4) coupled to the loss cavity (M1-M2) with QWP (quarter wave plate) and also to the mechanical mode  $b$  directly.

The second term is due to two field coupling between passive cavities (M1-M2) and (M1-M4) through quarter-wave plate (QWP),  $g$  is the coupling strength of the two-cavity modes and depends on the plate's rotated angle with respect to the crystal neutral axis. The third term is the coupling of the active and the passive cavities. The strength of photon-tunneling between the

active and passive cavities is denoted by  $J$  and can be tuned by changing the distance between the active and passive cavities. The fourth term is due to the laser inputs with Rabi frequency  $\Omega_j$  ( $j=1,2$ ). Both input at lasers have the same frequency and their polarizations are orthogonal. Although mean value of physical parameters is dependent on the Rabi frequencies, the small signal equations are independent on the Rabi frequency.

The Hamiltonian can be written in a rotating frame with frequency  $\omega_l$ .

$$H = \sum_{j=1}^3 (-\Delta_j a_j^\dagger a_j) + \omega_m b^\dagger b + \sum_{j=1}^2 G_j a_j^\dagger a_j (b + b^\dagger) + i \frac{g}{2} (a_1^\dagger a_2 - a_2^\dagger a_1) + J (a_1^\dagger a_3 + a_3^\dagger a_1) + \sum_{j=2}^3 \Omega_j (a_j + a_j^\dagger), \quad (3)$$

where the parameters  $\Delta_j = \omega_l - \omega_j$ ,  $j=1-3$  are cavities detuning frequencies. Equation 3 is employed to obtain the dynamic equations. In the presence of environmental losses and noises, the linearized quantum Langevin equations are:

$$\begin{aligned} \dot{a}_1 &= \left( i\Delta_1 - \frac{k_1}{2} \right) a_1 + \frac{g}{2} a_2 - iJ a_3 - iG_1 (b + b^\dagger) - \sqrt{k_1} a_{1in} \\ \dot{a}_2 &= \left( i\Delta_2 - \frac{k_2}{2} \right) a_2 - \frac{g}{2} a_1 - iG_2 (b + b^\dagger) - \sqrt{k_2} a_{2in} \\ \dot{a}_3 &= \left( i\Delta_3 + \frac{k_3}{2} \right) a_3 - iJ a_1 - \sqrt{k_3} a_{3in} \\ \dot{b} &= \left( -i\omega_m - \frac{\gamma_m}{2} \right) b - i \sum_{j=1}^2 G_j (a_j + a_j^\dagger) - \sqrt{\gamma_m} b_{in}, \end{aligned} \quad (4)$$

where  $\delta a_j$  ( $j=1,2,3$ ) and  $\delta b$  fluctuation are denoted by  $a_j$  and  $b$  respectively.  $a_{1in}$ ,  $a_{2in}$ ,  $a_{3in}$  and  $b_{in}$  are the noise operators with zero mean values and the correlation functions given by [21]:

$$\begin{aligned}\langle a_{i,in}^\dagger(t) a_{i,in}(t) \rangle &= 0 \\ \langle a_{i,in}(t) a_{i,in}^\dagger(t') \rangle &= \delta(t-t'), \quad i=1,2.\end{aligned}\quad (5)$$

Thermal reservoir of mechanical resonator is described by the damping  $\gamma_m$  and thermal occupation  $n_{th} = (e^{\hbar\omega_m/k_B T} - 1)^{-1}$ . The corresponding correlation functions are

$$\begin{aligned}\langle b_{in}^\dagger(t) b_{in}(t) \rangle &= n_{th} \delta(t-t') \\ \langle b_{in}(t) b_{in}^\dagger(t) \rangle &= (n_{th} + 1) \delta(t-t').\end{aligned}\quad (6)$$

The intrinsic quantum noise in the active cavity mode can be describe by the following correlation functions:

$$\begin{aligned}\langle a_{3in}^\dagger(t) a_{3in}(t) \rangle &= 0 \\ \langle a_{3in}(t) a_{3in}^\dagger(t') \rangle &= \delta(t-t').\end{aligned}\quad (7)$$

### III. COOLING RATE

The cooling rate of the mechanical resonator is calculated using the quantum noise spectrum of the optical force. The optical force operator can be written as follow:

$$F(t) = -\frac{\hbar G}{x_{zpf}} (a_1(t) + a_1^\dagger(t)). \quad (8)$$

By the Fourier transform of the autocorrelation function, the quantum noise spectrum of the optical force is introduced

$$S_{FF}(\omega) = \int dt e^{i\omega t} \langle F(t) F(0) \rangle. \quad (9)$$

Therefore, to obtain  $S_{FF}(\omega)$  we rewrite Eq. 4 in the frequency domain.

$$\begin{aligned}\frac{a_1(\omega)}{\chi_1(\omega)} &= -iJ a_3(\omega) - (g/2) a_2(\omega) - \\ &\quad - iG_1(b + b^\dagger) - \sqrt{k_1} a_{1in}(\omega) \\ \frac{a_2(\omega)}{\chi_2(\omega)} &= -(g/2) a_1(\omega) - iG_2(b + b^\dagger) - \\ &\quad - \sqrt{k_2} a_{2in}(\omega) \\ \frac{a_3(\omega)}{\chi_3(\omega)} &= -iJ a_1(\omega) - \sqrt{k_3} a_{3in}(\omega)\end{aligned}$$

$$\frac{b(\omega)}{\chi_b(\omega)} = -i \sum_{j=1}^2 G_j (a_j + a_j^\dagger) - \sqrt{\gamma_m} b_{in}(\omega), \quad (10)$$

where, the response functions  $\chi_j (j=1,2,b)$  are

$$\chi_j(\omega) = \frac{1}{-i(\omega + \Delta_j) + k_j/2}; \quad j=1,2,b, \quad (11)$$

where  $\Delta_b = -\omega_m$  and  $k_m = \gamma_m$ . By taking the Hermitian conjugate of both side of Eq. 10 Three new algebraic equations are obtained. The new equations and Eq. 10 made a system of linear algebraic equations with eight unknowns  $(a_1, a_2, a_3, b, a_1^\dagger, a_2^\dagger, a_3^\dagger, b^\dagger)$  and eight linear equations are algebraic. The system of linear algebraic equations versus noise function  $(a_{1in}, a_{2in}, a_{3in}, b_{in}, a_{1in}^\dagger, a_{2in}^\dagger, a_{3in}^\dagger, b_{in}^\dagger)$  are solved easily.  $a_1(\omega)$  and  $a_1^\dagger(\omega)$  are obtained, which are linear versus the noise functions. The noise functions are uncorrelated. Employing the correlation functions Eqs. 5-7 and the Fourier transform the correlation functions of noises in the frequency domain are obtained.

$$\begin{aligned}\langle a_{3in}^\dagger(\omega) a_{3in}(\omega') \rangle &= \delta(\omega + \omega') \\ \langle a_{3in}(\omega) a_{3in}^\dagger(\omega') \rangle &= 0 \\ \langle a_{jin}^\dagger(\omega) a_{jin}(\omega') \rangle &= 0, \quad j=1,2 \\ \langle a_{jin}(\omega) a_{jin}^\dagger(\omega') \rangle &= \delta(\omega + \omega') \\ \langle b_{in}^\dagger(\omega) b_{in}(\omega') \rangle &= n_{th} \delta(\omega + \omega') \\ \langle b_{in}(\omega) b_{in}^\dagger(\omega') \rangle &= (n_{th} + 1) \delta(\omega + \omega').\end{aligned}\quad (12)$$

Equation 8 is written in the frequency domain and correlation function  $\langle F^\dagger(\omega') F(\omega) \rangle$  verses  $\langle a_1(\omega') a_1^\dagger(\omega) \rangle$  and  $\langle a_1^\dagger(\omega') a_1(\omega) \rangle$  is written in the following:

$$\begin{aligned}\langle F^\dagger(\omega') F(\omega) \rangle &= \frac{\hbar^2 G^2}{x_{zpf}^2} \left[ \langle a_1(\omega') a_1^\dagger(\omega) \rangle + \right. \\ &\quad \left. + \langle a_1^\dagger(\omega') a_1(\omega) \rangle \right],\end{aligned}\quad (13)$$

where  $a_1(\omega)$  and  $a_1^\dagger(\omega')$  are linear functions of noise terms. Since  $a_{jin}(\omega) \{j=1,2,3\}$  and  $b_{in}(\omega)$  are uncorrelated, the  $\langle F^\dagger(\omega') F(\omega) \rangle$

versus noise correlation function is linear versus the correlation function of input noises. The spectral density  $S_{FF}$  is given by

$$S_{FF}(\omega) = \int d\omega' \langle F^\dagger(\omega') F(\omega) \rangle. \quad (14)$$

By employing the noise correlation function of Eqs. 12-14, the following equation for  $S_{FF}(\omega)$  is obtained:

$$S_{FF}(\omega) = \frac{G_1^2}{x_{zpf}^2} \left( k_1 |\chi(\omega)|^2 + \frac{g^2}{4} k_2 |\chi(\omega)|^2 |\chi_2(\omega)|^2 + J^2 k_3 |\chi(-\omega)|^2 |\chi_3(-\omega)|^2 \right), \quad (15)$$

where  $\chi(\omega)$  is the total system response function.

$$\chi(\omega) = \frac{\chi_{PT}}{1 + \chi_{PT} \left\{ \left[ \chi_2 (g G_2 / 2) + G_1 \right] + G_1^2 \chi_b \right\}}. \quad (16)$$

The response function of PT system is:

$$\chi_{PT}(\omega) = \frac{\chi_g}{1 + g^2 \chi_3 \chi_g}, \quad (17)$$

where,

$$\chi_g(\omega) = \frac{\chi_1}{1 + (g^2/4) \chi_2 \chi_1}. \quad (18)$$

In the overall the system function  $\chi(\omega)$  has a zero at the resonance frequency of (M1-M4) cavity i.e., we have a destructive interference at the resonance frequency of (M1-M4) cavity.

The rate of the mechanical resonator cooling is the difference between the rate of the anti-stokes,  $A_{as} = (x_{zpf}^2 / \hbar^2) S_{FF}(\omega_m)$  and stokes,  $A_s = (x_{zpf}^2 / \hbar^2) S_{FF}(-\omega_m)$  modes. For positive cooling rate,  $A_{as}$  should be larger than the heating rate  $A_s$ , which means the effective cooling rate parameter,  $\Gamma_{op} = A_{as} - A_s$ , is greater than zero. It is assumed that the resonance frequency is the same as stokes frequency. The parameters of the PT-symmetric resonator are chosen such that the resonance frequency is at the stokes frequency. The input noise does not affect the micromechanical resonator evolution. Since the resonance frequency of PT-

symmetric resonator is real value and completely noise destructive interference appears in the field-driven of the micromechanical resonator. At the exception point there is a phase transition in the PT-symmetry that the optical field is strongly localized in the gain cavity [28]. The optimized cooling rate occurs at the transition point, and the energy localization effect can be used to improve the cooling rate. The absorption rate of the anti-stokes photons can be increased. Therefore, the phase transition point for the best cooling rate is calculated:

$$J = \sqrt{\frac{k^2}{4} + \frac{G_1^2 k}{\gamma_m} + \frac{g^2 k}{4k_2} + \frac{gkG_1G_2}{k_2\gamma_m}}. \quad (19)$$

#### IV. GROUND-STATE COOLING IN THE BAD CAVITY

In this section, the cooling limit of the mechanical resonator is calculated at the steady-state. Therefore, the rate equation is solved in the steady-state ( $\dot{\bar{n}} = 0$ ,  $\bar{n}$  is the mean value of the phonon number state). The final mean phonon number  $n_f$  becomes [23]:

$$\bar{n}_f = \frac{\gamma_m n_{th} + A_s}{\gamma_m + \Gamma_{opt}}. \quad (20)$$

Total mean photon number includes two parts: the classical,  $\bar{n}_f^c = \frac{\gamma_m n_{th}}{\Gamma_{op} + \gamma_m}$ , and quantum,  $\bar{n}_f^q = \frac{A_s}{\Gamma_{op} + \gamma_m}$ , cooling limit.

The optimal cooling limit is obtained with the minimum  $\bar{n}_f$ , when  $\bar{n}_f < 1$ . The frequency of equality of gain and loss cavity is located at the stokes frequency  $\Delta_2 = \omega_m$  that causes vanishing of the intensity at stokes frequency and can cool the mechanical resonator.

Here, the mechanical frequency is  $\omega_m/2\pi = 20\text{MHz}$  and mechanical damping is  $\gamma_m = 10^{-5}$ . In our calculation the physical parameters,  $\Delta_1 = \Delta_3 = -\omega_m$ ,  $\Delta_2 = \omega_m$  and  $g = 0.1\omega_m$  are employed. The spectral density  $S_{FF}(\omega)$  versus normalized frequency  $\omega/\omega_m$  for different physical parameters are depicted in Figs. 2 and 3. The physical parameters of Figs. 2 and 3 are ( $k_1 = \omega_m$ ,  $G_1 = 0.005\omega_m$ ,

$G_2=0.0005\omega_m$ ) and ( $k_1=\omega_m$ ,  $G_1=0.01\omega_m$ ,  $G_2=0.001\omega_m$ ) respectively.

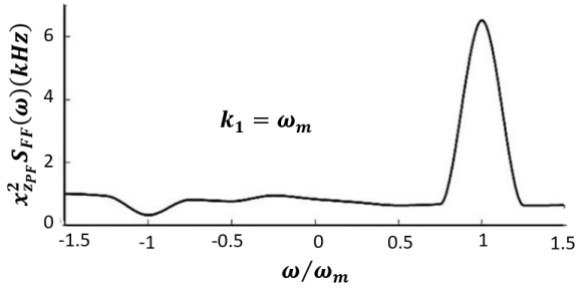


Fig. 2. The optical force spectrum  $S_{FF}(\omega)$  versus  $\omega/\omega_m$ . The other parameters are:  $G_1=0.005\omega_m$ ,  $G_2=0.0005\omega_m$ ,  $k_1=\omega_m$ ,  $k_2=0.5\omega_m$ ,  $g=0.1\omega_m$ .

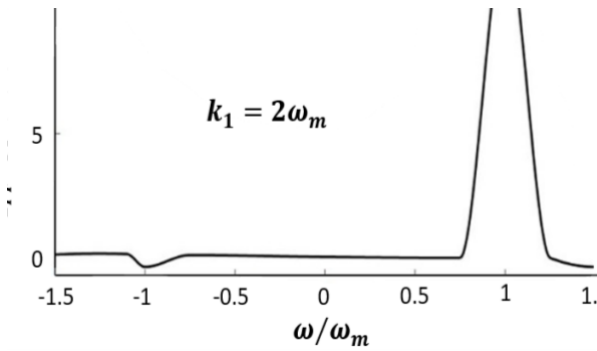


Fig. 3. The optical force spectrum  $S_{FF}(\omega)$  versus  $\omega/\omega_m$ . The other parameters are  $G_1=0.01\omega_m$ ,  $G_2=0.001\omega_m$ ,  $k_1=\omega_m$ ,  $k_2=0.5\omega_m$ , and  $g=0.1\omega_m$ .

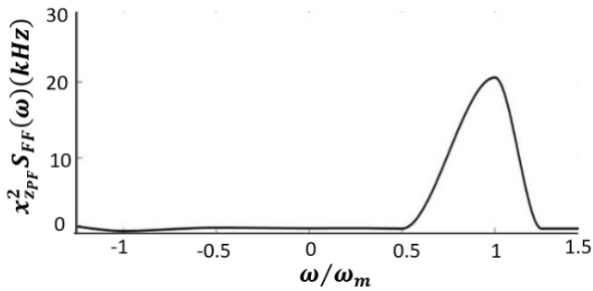


Fig. 4. The Optical force spectrum  $S_{FF}(\omega)$  versus  $\omega/\omega_m$ . The other parameters are  $G_1=0.01\omega_m$ ,  $G_2=0.001\omega_m$ ,  $k_1=2\omega_m$ ,  $k_2=0.5\omega_m$ , and  $g=0.1\omega_m$ .

Comparison of the results presented in Figs. 2 and 3 show that the minimum mean final phonon numbers are  $n_{f,min}=0.15$  and  $n_{f,min}=0.015$ , respectively. It seems that increasing the optomechanical coupling strength leads to enhanced cooling rate. Increasing  $G_1$  and  $G_2$  affects  $J$  and changes the phase transition point of the PT-symmetric optical cavities.

The spectral density of a bad cavity and ground state cooling of a bad cavity is resented in Fig.

4. The minimum final mean phonon number via  $G_1$  is plotted in Fig. 5. This figure shows that the blue and red detuning regimes have different behavior. Variation of final mean phonon number with respect to the  $g/\omega_m$  variation is shown in Fig. 6.

There is a gap between the blue and red detuning region. On the other hand, there exist the upper and lower limits of  $g/\omega_m$  for reaching the ground-state cooling.

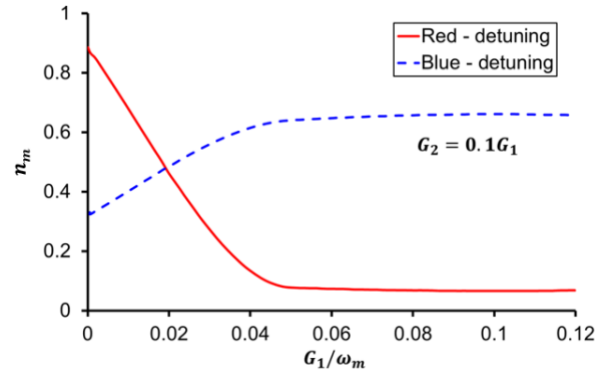


Fig. 5. Minimum phonon number  $n_m$  versus normalized optomechanical coupling coefficient,  $G_1/\omega_m$ , for red ( $\Delta_1=-\omega_m$ ) and blue ( $\Delta_1=\omega_m$ ) detuning and in both cases  $\Delta_2=-\Delta_1$ . The other parameters are:  $k_1=\omega_m$ ,  $k_2=0.1\omega_m$ , and  $g=0.5\omega_m$ .

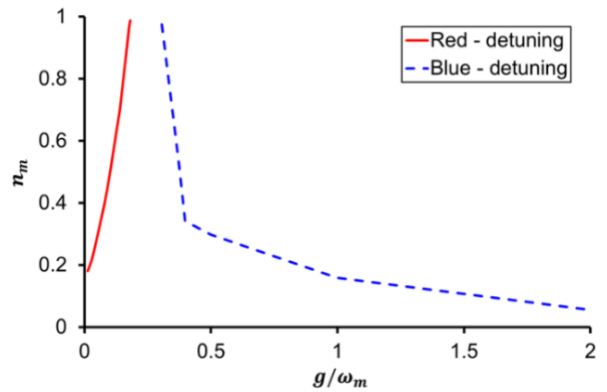


Fig. 6. Minimum phonon number  $n_m$  versus normalized optomechanical coupling coefficient,  $g/\omega_m$ , for red ( $\Delta_1=-\omega_m$ ) and blue ( $\Delta_1=\omega_m$ ) detuning and in both cases  $\Delta_2=-\Delta_1$ . The other parameters are:  $k_1=\omega_m$ ,  $k_2=0.1\omega_m$ ,  $G_1=0.005\omega_m$ , and  $G_2=0.0005\omega_m$ .

For example, for  $k_1=\omega_m$ ,  $k_2=0.1\omega_m$  and  $G_1=0.005\omega_m$ ,  $G_2=0.0005\omega_m$  the upper level of  $g/\omega_m$  in the red detuning is 0.18 and the lower level in blue detuning is 0.3. Figures 7 and 8 illustrate the minimum phonon number against normalized detuning  $\Delta_1/\omega_m$  for good cavity and bad cavity respectively. An important point is related to the weak optomechanical coupling.

It is worth noting in the experimental view because the generation of the strong coupling regime in the optomechanical system is very hard. The other advantage is about the bad cavity configuration of the optomechanical cavity. The results show, this system can do in the bad cavity limit as well in good cavity regime. In this system, the cavity that is directly related to the mechanical resonator decays at a fast rate while PT cavities decay at a slow rate, i.e., in the  $k_1 \gg k_2$  regimes of operation. In [16], fast ground-state cooling has been done for a bad cavity, but in our scheme, the ground-state cooling is done more efficiently, and the minimum phonon number was less. In [24], ground state cooling has been done by utilizing PT-system properties, but in our proposed method, ground-state cooling for bad cavity optomechanical systems is also possible.

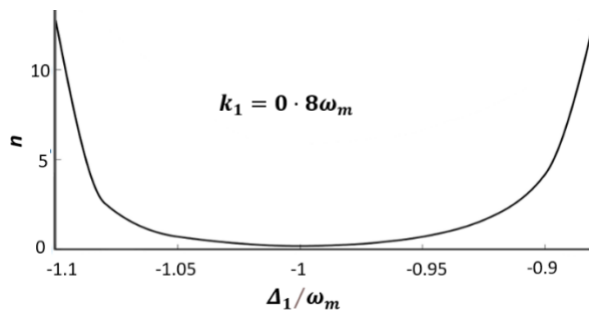


Fig. 7. The mean phonon number  $n$  versus normalized cavity detuning frequency,  $\Delta_1/\omega_m$ , with  $k_1=0.8\omega_m$ ,  $k_2=0.5\omega$  and  $\Delta_2=\omega_m$  for weak coupling  $G_1=0.005\omega_m$ ,  $G_2=0.0005\omega_m$ , and  $g=0.1\omega_m$ .

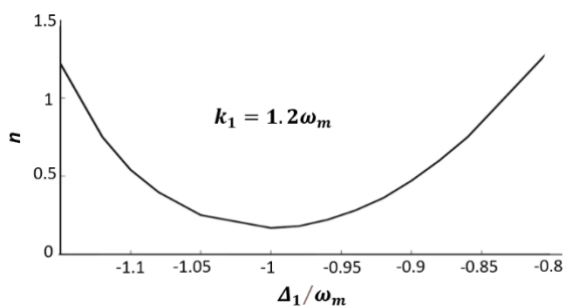


Fig. 8. Phonon number  $n$  versus normalized cavity detuning frequency,  $\Delta_1/\omega_m$ , with  $k_1=1.2\omega_m$  and the other parameters are the same as Fig. 7.

## V. CONCLUSION

The collaboration of a PT-symmetric resonator in a bad cavity causes the elimination of stokes frequency in the optomechanical system. The spontaneous emission noise of the active cavity is filtered by completely destructive noise

interference in the PT-symmetric resonator cavity. The main goal is optomechanical ground state cooling. Optomechanical coupling and decay rates of the cavities affect the optimal condition of mechanical cooling. The frequency of equality of gain and loss is located at stokes frequency, and the frequency of the optomechanical cavity is the anti-stokes frequency. Two effects were employed to improve the cooling in the optomechanical system. 1: The energy-localization mechanism near the exceptional point leads to the heat absorption from the mechanical resonator by the PT symmetric cavity. 2: The destructive quantum interference between two optical modes suppresses the heating process. We have designed a system in such a way that both effects can be applied simultaneously. The system consists of the gain cavity, which is coupled to the optomechanical cavity, and also of the quarter-wave plate that provides the linear mixing between the optomechanical cavity and the second passive optical cavity. The phase transition occurs at the exceptional point is calculated. It is shown that the optimal cooling rate is at this point. The minimum of the mean phonon number with respect to the optomechanical coupling strength and the coupled coefficient between the optical modes is investigated. The results show that the proposed system introduced in this system, works in a bad-cavity limit and weak optomechanical coupling regime. Also, the cooling rate is investigated in two regimes of operation. When the system is red-detuned with respect to the optomechanical frequency, by increasing the  $G_1$  parameter, the phonon number is decreased. The results display that the cooling can be attained in the bad-cavity limit of the optomechanical system. The other regime is blue-detuning where the large value of the  $G_1$  increases the minimum phonon number. The energy-localization reduces the coupling strength for achieving the ground state cooling in the red-detuned regime.



## REFERENCES

- [1] T.J. Kippenberg and K.J. Vahala, "Cavity optomechanics: back-action at the mesoscale," *Science*, Vol. 321, PP. 1172-1176. 2008.
- [2] P. Meystre, "A short walk through quantum optomechanics," *Annalen der Physik*, Vol. 525, pp. 215-233, 2013.
- [3] I. Favero and F. Marquardt, "Focus on optomechanics," *New J. Phys.*, Vol. 16, pp. 085006 (1-8), 2014.
- [4] F.Y. Khalili and S.L. Danilishin, "Quantum opto mechanics," *Prog. Opt.*, Vol. 61, pp. 113-236. 2016.
- [5] W.P. Bowen and G.J. Milburn, *Quantum opt mechanics*, CRC Press, 2015.
- [6] F. Marquardt, A.A. Clerk, and S.M. Girvin, "Quantum theory of optomechanical cooling," *J. Mod. Opt.*, Vol. 55, PP. 3329 -3338, 2008.
- [7] Y.C. Liu, Y.W. Hu, C.W. Wong, and Y.F. Xiao, "Review of cavity optomechanical cooling," *Chin. Phys. B*, Vol. 22, PP. 114213 (1-32), 2013.
- [8] Y.C. Liu, R.S. Liu, C.H. Dong, Y. Li, Q. Gong, and Y.F. Xiao, "Cooling mechanical resonators to the quantum ground state from room temperature," *Phys. Rev. A*, Vol. 91, PP.013824 (1-6), 2015.
- [9] H.K. Lau and A.A. Clerk, "Ground-state cooling and high-fidelity quantum transduction via parametrically driven bad-cavity optomechanics," *Phys. Rev. Lett.*, Vol. 124, PP. 103602 (1-7). 2020.
- [10] F. Farman and A.R. Bahrapour, "Heat transfer between micro-and nano-mechanical systems through optical channels," *J. Opt. Soc. Am. B*, Vol. 31, PP. 1525-1532, 2014.
- [11] F. Marquardt, J.P. Chen, A.A. Clerk, and S.M. Girvin, "Quantum theory of cavity-assisted sideband cooling of mechanical motion," *Phys. Rev. Lett.*, Vol. 99, PP. 093902 (1-5), 2007.
- [12] R. Riviere, S. Deleglise, S. Weis, E. Gavartin, O. Arcizet, A. Schliesser, and T.J. Kippenberg, "Optomechanical sideband cooling of a micromechanical oscillator close to the quantum ground state," *Phys. Rev. A*, Vol. 83, PP. 063835 (1-12), 2011.
- [13] Y.C. Liu, Y.F. Xiao, X. Luan, and C.W. Wong, "Dynamic dissipative cooling of a mechanical resonator in strong coupling optomechanics," *Phys. Rev. Lett.*, Vol. 110, PP. 153606 (1-6), 2013.
- [14] J. S. Bennett, L.S. Madsen, M. Baker, H. Rubinsztein-Dunlop, and Warwick P Bowen, "Coherent control and feedback cooling in a remotely coupled hybrid atom-optomechanical system," *New J. Phys.*, Vol. 16, PP. 083036 (1-27), 2014.
- [15] Y.C. Liu, Y.F. Xiao, X. Luan, and C.W. Wong, "Optomechanically-induced-transparency cooling of massive mechanical resonators to the quantum ground state," *Science China Phys., Mech. Astron.*, Vol. 58, PP. 1-6, 2015.
- [16] W.J. Gu and G.X. Li, "Quantum interference effects on ground-state optomechanical cooling," *Phys. Rev. A*, Vol. 87, PP. 025804 (1-6), 2013.
- [17] C. Chen, L. Jin, and R.B. Liu, "Sensitivity of parameter estimation near the exceptional point of a non-Hermitian system," *New J. Phys.*, Vol. 21, PP. 083002 (1-16), 2019.
- [18] Z.X. Yang, L. Wang, Y.M. Liu, D.Y. Wang, C.H. Bai, S. Zhang, and H.-F. Wang, "Ground state cooling of magnomechanical resonator in PT-symmetric cavity magnomechanical system at room temperature," *Frontiers Phys.*, Vol. 15, PP. 1-10, 2020.
- [19] H. Jing, S.K. Özdemir, X.Y. Lü, J. Zhang, L. Yang, and F. Nori, "PT-symmetric phonon laser," *Phys. Rev. Lett.*, Vol. 113, PP. 053604 (1-8). 2014.
- [20] X.Y. Lü, H. Jing, J.Y. Ma, and Y. Wu, "P T-symmetry-breaking chaos in optomechanics," *Phys. Rev. Lett.*, Vol. 114, PP. 253601 (1-5), 2015.
- [21] X. Bian, Y. Zhang, Z. Zhai, H. Yu, F. Zuo, G. Chen, and C. Jiang, "Enhanced four-wave mixing in P T-symmetric optomechanical systems," *Opt. Express*, Vol. 28, PP. 9049-9061, 2020.
- [22] Y.L. Liu and Y.X. Liu, "Energy-localization-enhanced ground-state cooling of a mechanical resonator from room temperature in optomechanics using a gain cavity," *Phys. Rev. A*, Vol. 96, PP. 023812 (1-15), 2017.
- [23] H. Xu, L. Jiang, A.A. Clerk, and J. Harris, "Nonreciprocal control and cooling of phonon modes in an optomechanical system," *Nature*, Vol. 568, PP. 65-69, 2019.



- [24] B. Peng, Ş.K. Özdemir, S. Rotter, H.Yilmaz, M. Liertzer, F. Monifi., C.M. Bender, F. Nori, and L. Yang, "Loss-induced suppression and revival of lasing," *Science*, Vol. 568, PP. 328-332, 2014.
- [25] B. Peng, Ş.K. Özdemir, F. Lei, F. Monifi, M. Gianfreda, G.L. Long, S. Fan., F. Nori, C.M. Bender, and L. Yang, "Parity-time-symmetric whispering-gallery microcavities," *Nat. Phys.*, Vol. 10, PP. 394-398, 2014.
- [26] L. Chang, X. Jiang, S. Hua, C. Yang, J. Wen, L. Jiang, G. Li, G. Wang, and M. Xiao "Parity-time symmetry and variable optical isolation in active-passive-coupled microresonators," *Nat. Photon.*, Vol. 8, PP. 524-529, 2014.
- [27] J. Zhang, B. Peng, S.K. Özdemir, Y.X. Liu, H. Jing, X.Y. Lü, Y.L. Liu, L. Yang, and F. Nori, "Giant nonlinearity via breaking parity-time symmetry: A route to low-threshold phonon diodes," *Phys. Rev. B*, Vol. 92, PP. 115407 (1-16), 2015.



**Zohre Mahmoudi Meimand** was born in Rafsanjan, Iran. She received her B.Sc. and M.Sc. degrees from Physics Department of Shahid Bahonar University of Kerman in 2004 and 2008, respectively. Now she is a PhD candidate in Shahid Bahonar University of Kerman. Her research interest includes quantum mechanics and quantum technologies.



**Omid Hamidi-Ravari**, born in Abadan, Iran, received his B.Sc. from Shahid Bahonar University of Kerman in 1988, his M.Sc. from Shiraz University in 1991 and his Ph.D. from McGill University, Montreal, Canada. He is a lecturer in Bahonar University since 1997.

His research interests include solvable quantum mechanical models, both relativistic and non-relativistic ones as well as quantum optical models. He is also interested in the application of orthogonal polynomials in quantum mechanics.



**Ali Reza Bahrampour** is a professor of physics at Physics Department of Sharif University of Technology. He received his B.Sc. and M.Sc. degrees from Electrical Engineering Department of Sharif University of Technology in 1974 and 1977, respectively. He received his PhD in mathematics from Shahid Bahonar University in 1988.

Now his research interest includes foundations of quantum mechanics and quantum technologies.

**THIS PAGE IS INTENTIONALLY LEFT BLANK.**